*32nd EPS Conference on Plasma Phys. Tarragona, 27 June - 1 July 2005 ECA Vol.**29C**, P-2.145 (2005)*

Effects of thermal electron motion on characteristics of discharges sustained by the Trivelpiece-Gould mode

Suwon Cho

Department of Physics, Kyonggi University, Suwon, Korea

Introduction

The high efficiency of plasma production in a magnetic field has increased interest for the discharge sustained by the Trivelpiece-Gould (TG) mode[1]. Modeling of the TG mode-sustained plasmas has been done by several researchers, but the electron temperature has not been considered. Recently, it has been shown that the electron thermal motion could modifies the dispersion characteristics and its influence is closely related to the radial density profile and the column radius in addition to the electron temperature and the collision frequency[2]. Since the magnetic field increases the inhomogeneity of the density profile in the perpendicular direction, the thermal motion could be more important for a magnetized plasma. This paper presents the electron temperature effects on characteristics of discharges sustained by the Trivelpiece-Gould mode.

Governing equations

We consider a cylindrical plasma column produced in a glass tube, whose inner and outer radii are R and R_1 respectively, with vacuum and a metal enclosure of the inner radius R_2 outside. It is supposed that an azimuthally symmetric wave is launched by an external source and the magnetic field is applied in the direction of the symmetrical axis ($B_0\hat{z}$). The plasma current is obtained from the electron momentum equation and is related to the electric and magnetic fields through the Maxwell equations, which yield

$$\frac{d\mathscr{E}_r}{d\xi} = \rho - \frac{\mathscr{E}_r}{\xi} - \kappa\mathscr{E}_z, \tag{1}$$

$$\frac{d\mathscr{E}_z}{d\xi} = -\mathscr{H}_\theta - \kappa\mathscr{E}_r, \tag{2}$$

$$\frac{d\mathscr{E}_\theta}{d\xi} = -\frac{\mathscr{E}_\theta}{\xi} + \mathscr{H}_z, \tag{3}$$

$$\eta\gamma_e\delta\frac{d\rho}{d\xi} = \frac{d\ln f}{d\xi}\eta\delta\rho + \left(\Omega_p^2\delta f + \Omega_c^2 - \delta^2\right)\mathscr{E}_r + \Omega_p^2\Omega_c f\mathscr{E}_\theta - \left(\delta^2 - \Omega_c^2\right)\kappa\mathscr{H}_\theta, \tag{4}$$

$$\frac{d\mathscr{H}_\theta}{d\xi} = -\frac{\kappa}{\delta}\eta\gamma_e\rho + \left(1 - \frac{\Omega_p^2 f}{\delta}\right)\mathscr{E}_z - \frac{\mathscr{H}_\theta}{\xi}, \tag{5}$$

$$\delta\frac{d\mathscr{H}_z}{d\xi} = \Omega_c\mathscr{E}_r + \left[\Omega_p^2 f + \delta\left(\kappa^2 - 1\right)\right]\mathscr{E}_\theta + \Omega_c\kappa\mathscr{H}_\theta, \tag{6}$$

with $r = \lambda\xi$, $\lambda = c/\omega$, $\kappa = k\lambda$, $\delta = 1 + i\nu_e/\omega$, $\eta = v_{te}^2/c^2$, $\rho = \rho_1\lambda/\varepsilon_0$, $\Omega_p = \omega_{pe}/\omega$, $\Omega_c = \omega_{ce}/\omega$, $\mathscr{E}_r = E_r$, $\mathscr{E}_\theta = iE_\theta$, $\mathscr{E}_z = iE_z$, $\mathscr{H}_r = iH_r/\varepsilon_0 c$, $\mathscr{H}_\theta = -H_\theta/\varepsilon_0 c$, $\mathscr{H}_z = -H_z/\varepsilon_0 c$, where ω_{ce} and ω_{pe} are the electron cyclotron and plasma frequencies, respectively, ν_e is the electron-neutral collision frequency for momentum transfer, v_{te} is the electron thermal speed, c is the speed of light in vacuum, ε_0 is the permittivity of the free space, ρ_1 is the perturbed charge density, and γ_e is the ratio of specific heats. Here, the spatial dependence of $\exp[i\int k(z)dz]$ is assumed. The wave equations with the relevant boundary conditions lead to an eigenvalue equation, which is solved to obtain $k(\equiv \beta + i\alpha)$ for a given value of ω/ω_{pe}. The procedure is described in detail for an unmagnetized plasma in Ref. [2] and it is extended to include the magnetic field.

The axial profile of the density can be found from the particle and power balance equations with the axial damping rate α[1, 3, 4]. Considering a long plasma column, the longitudinal diffusion is neglected compared to the transverse diffusion. It is also assumed that the diffusion is ambipolar and the absorbed wave energy is dissipated locally by collisions. Taking $n(r) = n_0 J_0(\mu r/R)$, where J_0 is the Bessel function of order 0, T_e and μ are determined from the Bohm condition at the sheath and the relation $T_e = -U_*/\ln[\Theta/\Theta_0]$. Finally, the axial profile of the plasma density is obtained from

$$\frac{dn}{dz} = -\frac{2\alpha n}{1 - \frac{n}{\alpha}\frac{d\alpha}{dn} + \frac{n}{\Theta}\frac{d\Theta}{dn}}, \tag{7}$$

where $\Theta = \nu_* U_*$, $\Theta_0 = \nu_*^0 U_*$, $\nu_* = \nu_*^0 e^{-U_*/T_e}$, U_* and ν_* are the excitation energy and frequency, respectively, and ν_*^0 is a slowly varying function of T_e.

Results

For illustration of the results, numerical calculations are conducted for an Argon plasma with the following parameters: the relative dielectric constant of the tube $\varepsilon_d = 3.78$, the plasma column radius $R = 10$ mm, the outer radius of the tube $R_1 = 11$ mm, the conductor boundary radius $R_2 = 30$ mm. At a fixed value of the wave frequency $\omega/2\pi = 2.45$ GHz, the plasma density is varied to obtain phase diagrams at the various values of the magnetic field and the pressure.

Figure 1 shows the phase diagram for cold and warm inhomogeneous plasmas. In addition to two turns of the phase diagram appearing in the cold plasma approximation, there are numerous turns in the warm plasma model and these are due to the combined effects of the thermal motion and collisions of the electrons. The temperature term also modifies the spatial damping rate near the cold resonance region, depending on the inhomogeneity of the radial density profile as compared in Figs. 1(a) and (b). At $\Omega_c = 0.2$ and $p = 0.2$ Torr, μ and T_e are found to be 2.12 and 2 eV, respectively, in which case the radial density profile is not steep enough for the electron

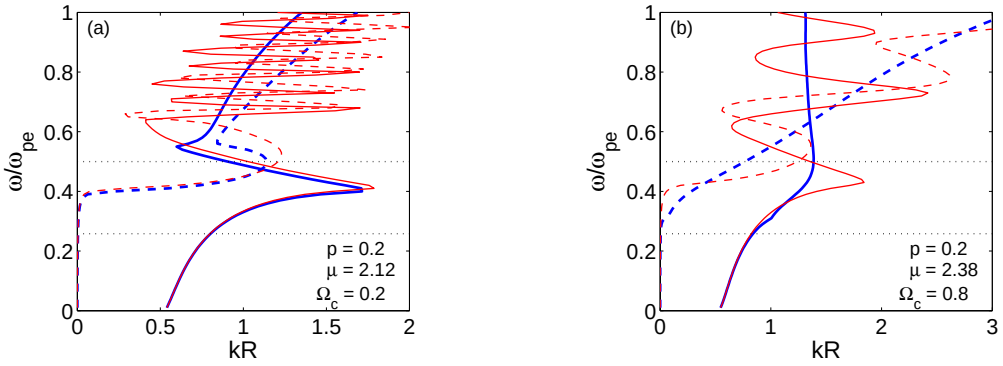

Figure 1: Variation of the wave number with the electron plasma frequency averaged over the radial axis when (a) $\Omega_c = 0.2$ and (b) $\Omega_c = 0.8$ at $p = 0.2$ Torr. The blue and red lines represent the results of the cold and warm plasma models, respectively, and the sold and dashed lines do the real and imaginary parts, respectively. The horizontal dotted lines are used to denote the onset and end points of a discharge given in Fig. 2.

temperature to make the difference in the damping rate and consequently in the axial density profile. Figure 2(a) presents the variation of the radially averaged value of the normalized density $N = \bar{n}/n_{\rm cr}$ ($n_{\rm cr} = \varepsilon_0 m_e \omega^2/e^2$) at $\Omega_c = 0.2$. At $\Omega_c = 0.8$, μ and T_e are estimated to be 2.38 and 1.6 eV, respectively, indicating that the inhomogeneity is quite strong and there is remarkable difference between the results of the cold and warm plasma models, as shown in Figs. 2(b).

A higher pressure can make the radial profile be steeper so that the magnetic field may not play a critical role in determining the inhomogeneity. An example is presented for the case of $p = 0.8$ Torr with the phase diagrams for $\Omega_c = 0.2$ and 0.8 shown in Fig. 3. Since the pressure is already high enough to lead a steep radial profile, the magnetic field has little effect on the inhomogeneity ($\mu = 2.30$ and 2.35) and consequently on the axial structure as given in Fig. 4. Finally, comparison of Figs. 2(a) and 4(a) reveals that for a weak magnetic field ($\Omega_c = 0.2$) the electron temperature influences the axial profile more significantly at 0.8 Torr than at 0.2 Torr, although the temperature is lower and the collision frequency is higher. This is because the inhomogeneity is stronger at a higher pressure, inferring that the inhomogeneity of the radial density profile is the important parameter of the thermal influence on dispersion and the axial structure, unless the collision frequency is too high and the temperature is too low.

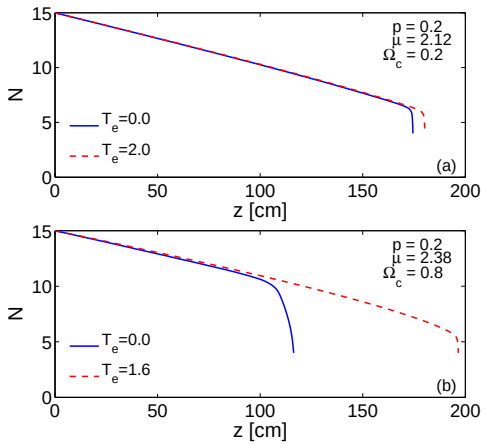

Figure 2: Axial profiles of the normalized density for (a) $\Omega_c = 0.2$ and (b) $\Omega_c = 0.8$ at $p = 0.2$ Torr, which correspond to the case of Fig. 1(a) and (b), respectively.

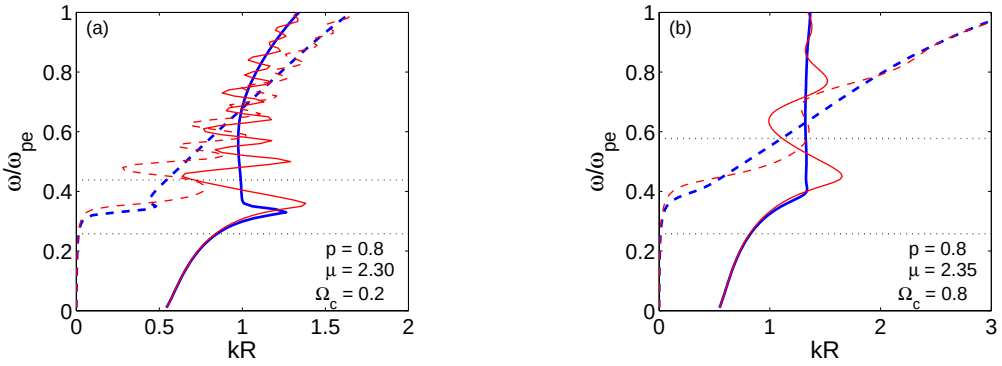

Figure 3: Variation of the wave number with the electron plasma frequency averaged over the radial axis when (a) $\Omega_c = 0.2$ and (b) $\Omega_c = 0.8$ at $p = 0.8$ Torr.

Conclusions

The thermal electron motion modifies the phase diagram as well as affects the axial density profile, and its influence is strongly related to the inhomogeneity of the radial density profile which is mainly controlled by the pressure and the magnetic field for a given geometry. Since the magnetic field increases the inhomogeneity of the radial density profile, the thermal effects can be more significant at a higher magnetic field when the pressure is low such that the density is not strongly inhomogeneous without the magnetic field. For weakly or unmagnetized plasmas the electron temperature influences the axial profile more significantly at a moderately high pressure due to the strong inhomogeneity of the radial profile, even though the temperature is lower and the collision frequency is higher.

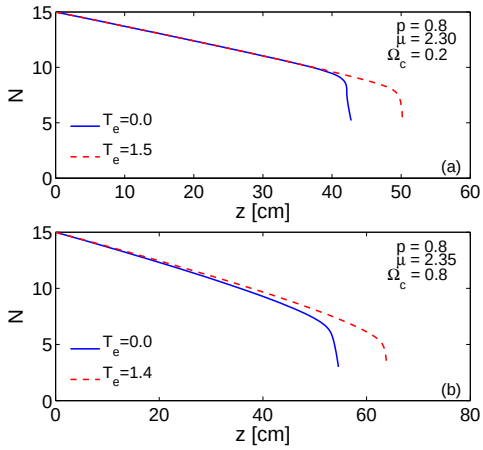

Figure 4: Axial profiles of the normalized density for (a) $\Omega_c = 0.2$ and (b) $\Omega_c = 0.8$ at $p = 0.2$ Torr, which correspond to the case of Fig. 3(a) and (b), respectively.

Acknowledgments

This work has been supported by Korea Basic Science Institute.

References

[1] H. Schlüter, A. Shivarova, and K. Tarnev, Contrib. Plasma Phys. **43**, 206 (2003).

[2] S. Cho, Phys. Plasmas **11** 4399 (2004).

[3] Y. M. Aliev, H. Schluter and A. Shivarova, *Guided-Wave-Produced Plasmas* (Springer, Berlin, 2000).

[4] K. Makasheva and A. Shivarova, Phys. Plasmas **8**, 836 (2001).